

# Journal Pre-proof

Analysis of decisive structural parameters of zeolites for alkylation of benzene with ethylene

Somayeh F. Rastegar, Galina Sadovska, Radim Pilar, Jaroslava Moravkova, Dalibor Kaucky, Libor Brabec, Jana Pastvova, Petr Sazama



PII: S0926-860X(19)30534-4  
DOI: <https://doi.org/10.1016/j.apcata.2019.117379>  
Reference: APCATA 117379  
To appear in: *Applied Catalysis A, General*  
Received Date: 4 September 2019  
Revised Date: 11 December 2019  
Accepted Date: 14 December 2019

Please cite this article as: Rastegar SF, Sadovska G, Pilar R, Moravkova J, Kaucky D, Brabec L, Pastvova J, Sazama P, Analysis of decisive structural parameters of zeolites for alkylation of benzene with ethylene, *Applied Catalysis A, General* (2019), doi: <https://doi.org/10.1016/j.apcata.2019.117379>

This is a PDF file of an article that has undergone enhancements after acceptance, such as the addition of a cover page and metadata, and formatting for readability, but it is not yet the definitive version of record. This version will undergo additional copyediting, typesetting and review before it is published in its final form, but we are providing this version to give early visibility of the article. Please note that, during the production process, errors may be discovered which could affect the content, and all legal disclaimers that apply to the journal pertain.

© 2019 Published by Elsevier.

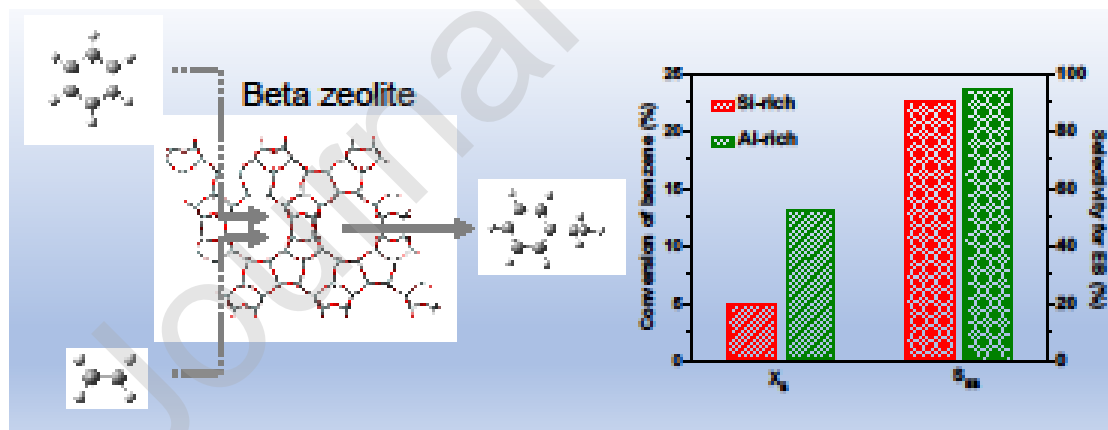
## Analysis of decisive structural parameters of zeolites for alkylation of benzene with ethylene

Somayeh F. Rastegar, Galina Sadovska, Radim Pilar, Jaroslava Moravkova, Dalibor Kaucky, Libor Brabec, Jana Pastvova, Petr Sazama\* [petr.sazama@jh-inst.cas.cz](mailto:petr.sazama@jh-inst.cas.cz)

J. Heyrovsky Institute of Physical Chemistry, Academy of Sciences of the Czech Republic, Dolejskova 3, 182 23 Prague, Czech Republic,

\*Corresponding author

### Graphical abstract



## Highlights

- The catalytic activity is controlled by the concentration of Brønsted acid sites.
- Channels sterically constrained for heavy by-products are decisive for selectivity.
- Lewis sites do not affect catalytic activity or selectivity.
- Superior activity and selectivity are obtained over Al-rich H-<sup>\*</sup>BEA zeolites.

## *Abstract:*

The effects of the zeolite structure and the Brønsted and Lewis sites on the activity and selectivity in alkylation of benzene with ethylene to ethylbenzene were investigated using three series of zeolites with different structures, Si/Al ratios and contents of Lewis sites. The 12-membered three-dimensional channels of beta zeolite (<sup>\*</sup>BEA) provide higher selectivity to ethylbenzene compared to faujasite zeolite (FAU) with cavities in which the di-alkylated and heavier by-products are formed. The activity is controlled by the concentration of Brønsted acidic sites, while Lewis sites do not contribute to the activity or affect the selectivity. The highest activity and selectivity are obtained using Al-rich H-<sup>\*</sup>BEA (Si/Al 4.2) with a high density of Brønsted groups in a well-defined channel structure sterically constrained for heavy by-products. It is shown that a three-dimensional channel structure with Brønsted acid sites in a shape selective environment is a key parameter controlling the activity and selectivity.

*Keywords: Alkylation of benzene; Ethylbenzene; Beta zeolite (<sup>\*</sup>BEA); Organotemplate-free Al-rich Beta; Mordenite (MOR); Faujasite (USY)*

## 1. Introduction

Due to the substantial increase in ethylbenzene (EB) production, an important petrochemical intermediate in styrene production, considerable effort has been exerted to find an efficient catalytic process which can conventionally produce EB [1]. EB is mostly synthesized by benzene (B) ethylation over acidic catalysts. Traditional processes were based on the use of strong mineral and Lewis acids, such as  $\text{H}_2\text{SO}_4$ ,  $\text{BF}_3$ , and HF. The emphasis on cleaner and safer technologies without the problematic handling, corrosion and waste disposal of these catalysts [2] has resulted in the development of faujasite (FAU, USY) zeolite alkylation catalysts effective in EB production in the liquid phase [3]. In the early 1990s, a patent by Chevron showed that, in the liquid-phase, the alkylation/transalkylation catalysis can be performed on a beta (\*BEA) zeolite [4]. Shortly after this, it was shown that MCM-22 zeolite can also be used as an active catalyst in benzene alkylation [5]. Although the catalytic activity of MCM-22 is comparable (with a lower deactivation rate) to USY, is still approximately 2.4 times less than \*BEA zeolite [5]. The strength and concentration of Brønsted acidic sites in the zeolites and the transport of the products from the inner channels of the zeolites are assumed to be responsible for the activity of zeolites in the alkylation reaction [1, 2, 4, 6-12]. The latter is predominantly governed by the size of the zeolite crystals and the kinetic diameters of the reactants and products [13] relative to the diameter of the zeolite channels (see Figure 1). It has been demonstrated that the shape selectivity of zeolite in alkylation/transalkylation is related to the geometry and dimensions of the internal channels [14]. For example, medium-sized pore ZSM-5 zeolites with 10-ring channel openings (pore diameter of about 0.55 nm) have been shown to be a suitable catalyst for the synthesis of para-dialkyl benzene isomers. However, the 12-ring channels in \*BEA zeolite do not exhibit para-selectivity but are advantageously used in the synthesis of monoalkyl benzenes, like

EB and isopropylbenzene. As the kinetic diameters of the alkylbenzene molecules are close to the diameter of the inner channels of \*BEA zeolite, the complex reaction mechanism and thus product composition are controlled by shape-selective effects [15]. In the absence of a product shape-selectivity effect, the monoalkylation of benzene is followed by the formation of other polyalkylates, since the benzene aromatic ring is activated in the presence of an alkyl group. Therefore, in order to obtain high EB selectivity, it is advisable to operate the process at a high benzene/ethylene ratio. On the other hand, the unfavourable polyalkylates produced in the alkylation process can be transalkylated back in the presence of benzene.

This work studies the relationships between the concentration and type of acid centres (Brønsted/Lewis) and their concentration on the catalytic activity in the alkylation of benzene to EB and selectivity to dialkylated products and by-products in the liquid phase on \*BEA zeolites, comparing the shape selectivity of \*BEA zeolites with that of a traditional USY zeolite catalyst. The study exploited the progress in the synthesis of Al-rich \*BEA zeolite [16-20], which enabled a significant increase in the concentration of Al in the zeolite framework, for the preparation of catalysts with a high concentration of Brønsted acid sites. The study analyses the effects of high concentrations of Brønsted and Lewis acid sites in Al-rich \*BEA zeolites on the catalytic activity and selectivity.

## 2. Experimental

### 2.1 Preparation of zeolites

The faujasite zeolite (CBV 712, Si/Al = 6) denoted as FAU/6, mordenite zeolite (CBV10 A, Si/Al 5.8) denoted as MOR/5.8 and high-silica \*BEA zeolites (CP814B, Si/Al 12.5 and CP814C, Si/Al 18) denoted as BEA/12.5 and BEA/18, respectively, were kindly provided by Zeolyst

International. Al-rich \*BEA zeolites with Si/Al ratios 4.2 and 4.8, denoted as BEA/4.2 and BEA/4.8, respectively, were obtained by hydrothermal syntheses performed using an organotemplate-free procedure at 140 °C. BEA/4.8 was synthesised using synthesis gel with a molar composition of 1 SiO<sub>2</sub> : 0.08 Al : 0.4 NaOH: 8.5 H<sub>2</sub>O. NaAlO<sub>2</sub> and Aerosil were used as sources of alumina and silica, respectively. BEA/4.2 was synthesised from synthesis gel with a molar composition 1 SiO<sub>2</sub> : 0.13 Al : 0.4 NaOH : 7.5 H<sub>2</sub>O prepared using Al(OH)<sub>3</sub> and Bindzil as sources of alumina and silica, respectively. Calcined beta zeolite (Si/Al 10, Zeolyst International) was added in the amount of 10 wt.% to the suspension of the aluminosilicate gel to act as the seeds in the both synthesis procedures. Al-rich \*BEA zeolites with Si/Al ratios 4.5 and 5, denoted as BEA/4.5 and BEA/5, respectively, were provided by Euro Support Manufacturing Czechia. All the zeolites were ion-exchanged three times with 100 ml 0.5 M NH<sub>4</sub>NO<sub>3</sub> solution for 12 h, filtered and dried at 70 °C overnight. The obtained ion-exchanged zeolites were typically calcined at 520 °C for 4 h to obtain the protonic form. Table 1 lists the zeolites used in this study.

## 2.2 *Characterization of zeolites*

X-ray diffraction analysis (XRD) was used to analyse the phase composition of powdered zeolites using a MiniFlex 600 (Rigaku, Japan) diffractometer equipped with a vertical goniometer (with goniometer accuracy of  $\pm 0.02^\circ$ ) in the  $2\theta$  range of  $10^\circ - 50^\circ$ . A copper anode (U = 40 kV, I = 15 mA) was used as a source of X-ray radiation. The textural properties of powders were analysed by adsorption isotherms of nitrogen at 77 K performed with a Micrometrics 3FLEX volumetric adsorption unit. All the samples were outgassed, before the adsorption experiment, at 400 °C for 24 h to purify the surface of the samples. Fitting the Broekhoff–de Boer t-plot was used to determine the volume of the micropores and the external

surface area. HR-TEM images were obtained by JEOL JEM-2100Plus high-resolution transmission electron microscope (HR-TEM) operated at 200 kV (LaB6 cathode, point resolution 1.9 Å). Dispersion of zeolite powder was cast on the lacey carbon copper grid and dried at 120 °C before inserting into the microscope. HR-SEM micrographs were obtained using a Hitachi S 4800-I field emission scanning electron microscope. The FTIR spectra of adsorbed  $d_3$ -acetonitrile were used to analyse the concentrations of the Brønsted and Lewis acid sites. The spectra were recorded at RT on a Nicolet Nexus 670 FTIR spectrometer operating at resolution of  $1\text{ cm}^{-1}$  by collecting 256 scans for each spectrum. The zeolites were evacuated at 450 °C for 180 min prior the adsorption of  $d_3$ -acetonitrile (10 mbar of  $\text{CD}_3\text{CN}$  at room temperature for 15 min with subsequent evacuation at room temperature for 15 min). The characteristic absorption bands of the  $\text{C}\equiv\text{N}$  vibrations and the extinction coefficients obtained in our previous study ( $\epsilon_{\text{B}} = 2.05\text{ cm}\ \mu\text{mol}^{-1}$  and  $\epsilon_{\text{L}} = 3.60\text{ cm}\ \mu\text{mol}^{-1}$ ) [21] were used to determine the concentrations of the acid sites. Competitive adsorption of benzene and EB was analysed on two Al-rich and Si-rich \*BEA zeolites. Benzene was adsorbed (18 Torr for 15 min) and subsequently EB was adsorbed (3 Torr for 15 min) at RT. Then the samples were evacuated for 30 min at RT. The procedure leads to the adsorption of benzene/EB at Brønsted sites and the absence of adsorbed molecules on silanols. Comparison of the intensity of the vibrations in the benzene rings and the vibrations of the ethyl groups provided information on the benzene/EB competitive adsorption on Si-rich and Al-rich \*BEA zeolites.

### **2.3 Analysis of catalytic properties**

Alkylation of benzene with ethylene was carried out in a 500 ml stirred batch reactor at a temperature of 180 °C with *n*-heptane as GC internal standard. To determine the activation

energy, the activity was also measured for selected samples in the 150 to 200 °C temperature range. The liquid mixture was washed twice with N<sub>2</sub> to remove O<sub>2</sub> and then 0.5 g of catalyst was added to the reactor. The catalysts were activated in the dryer at 220 °C/16 h (air) before adding to the reaction mixture. Ethylene was added to the reactor at 180 °C and the pressure was kept constant at 40 bar. The consumed ethylene was continuously replaced in the reactor to maintain a constant pressure. To suppress the formation of unwanted by-products, excess benzene is used in all the experiments (the benzene/ethylene molar ratio was kept at ~ 5). Samples for analysis were taken at 15 min intervals. Analysis of the products was carried out by a Perkin-Elmer Clarus 580 gas chromatograph equipped with a capillary CP-Sil PONA CB (100 m x 0.25 mm x 0.5 μm) column and a flame ionization detector (FID). The catalytic activity of each zeolite was defined in terms of conversion of benzene (X<sub>B</sub>), the yield of EB (Y<sub>EB</sub>) and selectivity of each product as follows:

$$\%X_B = \left(1 - \frac{N_B(t)}{N_B(t=0)} \times \frac{N_{H(t=0)}}{N_H(t)}\right) \times 100$$

$$\%Y_{EB(DEB)} = \left(\frac{N_{EB}(t) - N_{EB}(t=0)}{N_B(t=0)} \times \frac{N_{H(t=0)}}{N_H(t)}\right) \times 100$$

$$\%S_{EB(\text{other products})} = \left(-\frac{N_{EB}(t)}{(N_B(t) - N_B(t=0))} \times \frac{N_{H(t=0)}}{N_H(t)}\right) \times 100$$

Where the N stands for a number of moles of reactants or products, Y<sub>EB</sub> corresponds to the yield of EB (or DEB and heavier by-products) and S is the selectivity of EB, DEB, and other by-products. We used the appropriate kinetic tests to confirm that the reaction is not affected by mass transfer limitations. To analyse the possible effects of external diffusion, the catalytic test was performed on a very active catalyst BEA/5 at different stirring rates from 25 to 250 rpm using a U-type stirrer designed for intensive mixing of catalytic reactors. Practically identical conversions were achieved at a stirring rate of 100 - 250 rpm. On the basis of these results, the

activity was analysed for all the catalysts in this study using a stirring rate of 150 rpm. To determine the effect of intra-crystalline diffusion on the activity of \*BEA zeolites, we analysed the conversion of benzene and selectivity for EB, DEB and higher products for two Al-rich BEA/4.2 and BEA/4.5 zeolites of very similar compositions but with different crystal sizes of 0.4 - 0.5  $\mu\text{m}$  and 0.1 - 0.2  $\mu\text{m}$ , respectively. The same attained conversions of benzene clearly indicate the absence of the effect of intra-crystalline diffusion on the observed activities. Since BEA/4.2 is the sample with the largest crystals and the highest concentrations of active sites of all the beta zeolite samples used in the study, we can exclude the effect of intra-crystalline diffusion on the activity of the other \*BEA samples with smaller crystal size a lower concentrations of active sites.

### **3. Results and discussion**

#### **3.1 Structure of the zeolite catalysts**

Table 1 lists a series of \*BEA zeolites with molar Al/Si ratios from 4.2 to 18 and Al-rich MOR and USY zeolites with a similar molar ratio Al/Si  $\sim$  6 used for analysis of the effects of the Si/Al ratio and zeolite channel structure on the alkylation of benzene with ethylene, respectively. The XRD patterns and electron microscopic images of the zeolites are depicted in Figures 2 and 3. The characteristic patterns and intensities of the XRD lines, the microporous volumes  $\sim$  0.15 – 0.2  $\text{cm}^3.\text{g}^{-1}$  for \*BEA and MOR zeolites and  $\sim$  0.3  $\text{cm}^3.\text{g}^{-1}$  for USY, and the electron scanning images indicate a well-developed crystalline structure for all the parent zeolites. Al-rich \*BEA zeolites consist of well-defined crystals in the form of a truncated octahedron, Si-rich \*BEA consist of aggregates of small intergrown crystals and USY shows crystals with cubic morphology. The zeolite crystal size for all the samples is in the range from 0.1 to 1  $\mu\text{m}$ . A shift

in the intense XRD reflections of the Al-rich \*BEA zeolites  $\sim 0.4^\circ 2\theta$  to lower values with respect to the reflections of the Si-rich BEA/12 and BEA/18 samples reflects the higher concentration of Al in the zeolite framework. A detailed study of the distribution of Al atoms in the framework of Al-rich \*BEA zeolites and concentration and nature of related acidic sites was reported previously [22]. A detailed structural analysis of the MOR and USY samples has been described elsewhere [20, 23]. The previous  $^{27}\text{Al}$  MAS NMR studies on the \*BEA and MOR zeolite samples showed that aluminium is tetrahedrally coordinated in the framework without a significant signal for non-lattice aluminium.  $\text{Si}/\text{Al}_{\text{Fr}}$  values for the \*BEA and MOR zeolites obtained from the  $^{29}\text{Si}$  MAS NMR spectra are similar to those obtained from chemical analysis [20, 22].

### ***3.2 Analysis of activity and selectivity in benzene alkylation with ethylene***

#### ***3.2.1 Effect of the zeolite structure***

To understand the role of the channel structures in the alkylation of benzene with ethylene, conversion of benzene as a dependence on the reaction time over the Al-rich \*BEA, MOR and USY zeolites was analysed and plotted in Figure 4. Note that FAU, MOR, and \*BEA zeolites exhibit very similar framework composition and particle size and the catalytic activity was measured with the same pre-treatment and under identical reaction conditions. The figure shows that the conversion of benzene over the BEA/5 is significantly higher than for FAU/6 and MOR/5.8. The results indicate that the geometry and dimensionality of the channel system of the zeolites play a decisive role in their activity. The interaction of the reactant molecules in the confined reaction space with Brønsted acid sites and with the inner walls of the zeolite channels are factors controlling the reaction rate, where a more confined reaction space in the pore

structures and the higher acid strength and concentration of acid sites yield a higher reaction rate [24-26]. The Brønsted OH groups corresponding to Al-Si-Al sequences in the framework of FAU zeolites exhibit lower acid strengths compared to Al-rich \*BEA due to mutual interactions of close OH groups [20, 22, 27, 28]. The greater reactant confinement and the stronger van der Waals interactions in the interior of the \*BEA zeolitic channels compared to the FAU zeolite [29, 30] with relatively large inner cavities with a diameter of 1.2 nm together with the presence of a high concentration of acid sites in Al-rich \*BEA zeolite enable the alkylation reaction at ca 2.5 times higher rates compared to the FAU/6 zeolite. The very low activity of the MOR zeolite is associated with the diffusion-restricted accessibility of the acid sites in the 8-ring for C<sub>6</sub> molecules and mono-dimensional 12-ring channels in MOR lowering the efficiency of the catalytic process by mass transfer effects [23, 31]. Partial dealumination or desilication of Al-rich mordenite, which opens the side 8-ring channel pockets and re-organises the channel structure from mono-dimensional to three-dimensional, is necessary for improving the MOR activity in the alkylation reaction [32, 33].

Figure 4B shows a comparison of the selectivity of the FAU/6 and BEA/5 samples in EB, DEB, and heavier by-products at similar benzene conversions. FAU/6 zeolite produces more DEB and much heavier by-products (C ≥ 9) due to the lack of shape-selectivity in the supercages and three dimensional channel system with 0.74 x 0.74 nm openings accessible to large DEB isomers. High selectivity of the \*BEA zeolite is related to the well-defined sterically constrained environment of 12-membered three-dimensional channels (0.66 nm × 0.67 nm, 0.56 nm × 0.56 nm) which are readily accessible for benzene and EB, in which both the DEB isomers and heavier by-products barely diffuse out of the zeolite pores. Figure 1 illustrates the diameters of

the pore openings of the \*BEA and FAU zeolites and the kinetic diameters of benzene, EB, and three DEB isomers.

### 3.2.2 Effect of the Si/Al ratio

Figure 5A depicts the effect of the aluminium content in the \*BEA zeolites on the conversion in the alkylation of benzene with ethylene. Consistent with the reports of Bellussi et al. [6], Yilmaz et al. [19] and De Baerdemaek et al. [34], the conversion increases with an increasing amount of framework Al in the \*BEA zeolites. The conversion of benzene gradually increases with a decrease in the Si/Al ratios up to the maximum content of Al achievable by the zeolite synthesis, i.e. up to 4.2 in the Al-rich BEA/4.2 sample. A significant increase in the activity of Al-rich \*BEA zeolites (Si/Al 4 – 5) compared to Si-rich zeolites (Si/Al  $\geq 10$ ) was previously also observed in the hydroamination of aromatics [20], isomerization of alkanes [28, 35] and cracking and hydrocracking of aromatics and alkanes [20, 34, 36]. Both analysis of ammonia desorption and  $^1\text{H}$  MAS NMR and FTIR spectroscopy investigations [22, 28, 34, 37] of the concentration and acid strength of Brønsted sites in Al-rich \*BEA zeolites showed that the concentration of Brønsted sites is approximately proportional to the increased Al content in the framework without significant changes in their acid strength which is similar to the Brønsted sites in Si-rich \*BEA zeolites. The comparable apparent activation energies of  $\sim 70 \text{ kJ mol}^{-1}$  for Al-rich BEA/5 and Si-rich Al-rich BEA/12.5 and a higher pre-exponential factor for Al-rich BEA/5 compared to Si-rich Al-rich BEA/12.5 were obtained from the Arrhenius plots for the benzene alkylation reaction (Figure 5B). This is consistent with the higher concentration of the Brønsted active sites in the BEA/5 sample without marked change of their acidic properties. The previous studies on the structure of Al-rich \*BEA zeolites showed that a predominant part of the Al atoms in the

zeolite framework is located in Al-Si-Al sequences [22, 34, 38-40]; however in contrast, e.g., to the faujasite structure, these Al-Si-Al sequences form the zeolite wall separating two neighbouring channels. Al atoms of the Al-Si-Al sequence in Al-rich \*BEA thus face into two channels providing two non-interacting Brønsted OH groups located in different channels [22]. The deprotonation energies of these non-interacting Brønsted sites corresponding to Al-Si-Al in Al-rich are comparable with those for Al-Si<sub>n≥2</sub>-Al sequences in Si-rich \*BEA zeolites, indicating a similar strength of the acid sites [20]. The high Al concentration in the framework Al-rich \*BEA zeolites and the corresponding Brønsted centres with sufficient acid strength thus allow a significant increase in the activity compared to the hitherto most active Si-rich \*BEA zeolites. Recycling the BEA/5 catalyst three times showed no loss in conversion of benzene or selectivity for EB.

Figure 5C compares the selectivity of the Al-rich and Si-rich \*BEA zeolites. The selectivity for EB is slightly higher for the Al-rich \*BEA samples producing less DEB and heavier by-products compared to the Si-rich BEA/12.5 zeolite for similar conversion of benzene. Yilmaz et al. associated high selectivity towards the monoalkylated products in alkylation of benzene with the polarity of the zeolite framework increasing with the content of the aluminium [19]. High polarity of Al-rich \*BEA zeolite could favour adsorption of benzene over that of EB, which decreases subsequent alkylation reactions due to the higher rate of desorption of the EB product. We employed infrared spectroscopy to determine whether the greater polarity of Al-rich zeolites could, in fact, result in greater coverage of the acid sites with benzene. We adsorbed a mixture of benzene and EB on Si- and Al-rich \*BEA zeolites and observed the intensity of the absorption bands of the benzene ring and the ethyl group under conditions where benzene and EB are adsorbed predominantly on Brønsted sites (Figure 6). The spectra show higher relative

intensity of the adsorption bands corresponding to the benzene ring on the Al-rich \*BEA zeolite sample at the same intensity of the bands of the ethyl group on both zeolites. They clearly show slightly greater relative benzene coverage, which could be responsible for the greater selectivity for ethyl benzene during the alkylation reaction on Al-rich \*BEA zeolites. Direct evidence could be obtained by monitoring the adsorbed entities under the reaction conditions; however, analysis of the adsorbed molecules at high pressures and temperatures in the liquid phase is not experimentally feasible.

We could not exclude that the textural properties also contribute to the higher selectivity obtained over Al-rich \*BEA zeolites. Al-rich \*BEA consists of well-developed crystals (Figure 3, Table 1) with a much smaller external surface area, possibly implying high shape-selectivity effects of the defined reaction environment of the regular inner pores compared to small crystallites of Si-rich \*BEA zeolites with a large external surface (Table 1). We analysed the selectivity for EB, DEB and higher products at a conversion of ~15% for two Al-rich BEA/4.2 and BEA/4.5 zeolites of very similar compositions but with different crystal sizes of 0.4 - 0.5  $\mu\text{m}$  and 0.1 - 0.2  $\mu\text{m}$ , respectively. Figure 7 shows practically identical selectivity for EB for both samples. The larger and better developed crystals of BEA/4.2 did not significantly alter the reaction selectivity. It seems that the selectivity of Al-rich \*BEA zeolites is not significantly affected by the particle morphology and the external surface. This is consistent with the fact that, for most reactions acid catalysed by zeolites, the van der Waals interactions of the reacting molecule in the confined interior of the zeolitic channels and the presence of the acid sites in the environment of the channels are essential [35]. However, it cannot be excluded that the increase in the external surface area and the reduction of diffusional path lengths do not contribute to the

changes in the reaction selectivity when the crystal size is reduced below 100 nm for Si-rich \*BEA zeolites.

### 3.2.3 Effect of the concentration of Lewis and Brønsted acid sites in \*BEA zeolites

Compared to zeolites with other structural topologies, the \*BEA zeolite exhibits a greater tendency both to reversible and non-reversible changes in the coordination of the T atoms, especially aluminium, and to easier creation of the Lewis sites either in the form of the perturbed framework Al-defective sites or extra-framework Al species [20, 41]. Lewis sites play the role of active centres in many acid-catalysed reactions, affect the specific activity of the Brønsted sites, or influence the reaction mechanism and the selectivity of the reaction [42, 43]. The presence of Lewis sites in the close vicinity of Brønsted acid sites in zeolite catalysts was shown to increase the participation of hydrogen transfer reactions in the complex process of transformation of methanol to hydrocarbons (MTH) [44, 45] and in cracking of alkenes [46]. The pairs of Brønsted and Lewis acid sites in zeolite catalysts provided much higher reaction rates for alkane cracking [47-49]. In previous studies [1, 6, 7, 50], the activity in alkylation of benzene by ethylene over \*BEA zeolites was associated with the content of aluminium in the zeolite without analysing the nature of the acid sites. To assess the role of Brønsted and Lewis acid centres in the benzene alkylation reaction, a series of \*BEA zeolite samples was prepared by calcining BEA/4.8 at temperatures from 450 to 600 °C. The concentration and nature of acidic active sites in the series of BEA/4.8 zeolites calcined at the different temperatures and in the \*BEA zeolites with different Si/Al ratios were determined by  $d_3$ -acetonitrile adsorption monitored by FTIR spectroscopy.

The FTIR spectra of OH groups for the Al-rich and Si-rich \*BEA zeolites are shown in Figure 8A. The spectra in the region of the OH groups exhibit absorption bands characteristic of

the bridging OH groups with maxima at 3610 – 3614  $\text{cm}^{-1}$  and bands reflecting the presence of the silanol groups at 3745  $\text{cm}^{-1}$ . The increase in the intensity of the absorption band of the bridging OH groups for the Al-rich compared to the Si-rich zeolites is approximately proportional to the increase in the aluminium concentration in the zeolite. However, the absorption at 3610 – 3614  $\text{cm}^{-1}$  corresponds to only non-interacting bridging OH groups, while hydrogen-bonded silanols and Brønsted hydroxyls are associated with a broad background signal with a maximum at about 3500  $\text{cm}^{-1}$  [51]. The high intensity of the absorption bands for the terminal Si-OH groups for the Si-rich zeolites is given by the large external surface of the small crystal particles. No absorption bands were found in the 3650 – 3600  $\text{cm}^{-1}$  region, indicating the absence of Al–OH species for all the zeolite samples. Adsorption of  $d_3$ -acetonitrile resulted in the appearance of absorption bands at 2290 and 2325  $\text{cm}^{-1}$  corresponding to the  $\nu(\text{C}\equiv\text{N})$  stretching mode of  $d_3$ -acetonitrile adsorbed on Brønsted and Lewis sites, respectively (Figure 8B). The intensity of both the absorption bands obviously decreases with increasing Si/Al ratio. The results of quantitative analysis of the acid sites using the integral intensities of the absorption bands are summarised in table 2. They show that the concentrations of the acid sites correspond to the aluminium contents in all the zeolites with predominant Brønsted sites and significant concentrations of Lewis sites typical of \*BEA zeolites [52, 53].

The spectra of adsorbed acetonitrile on BEA/4.8 calcined at temperatures from 450 to 600 °C in figure 9A show a gradual decrease in the intensity of the absorption bands characteristic of the C≡N group interacting with the Brønsted sites at 2290  $\text{cm}^{-1}$  and an increase in the intensities of the bands of the Lewis-coordinated acetonitrile at 2325  $\text{cm}^{-1}$  with increasing calcination temperature. The dehydroxylation of the Brønsted groups occurred progressively with increasing calcination temperatures and led to the formation of the Lewis sites from 0.5

mmol.g<sup>-1</sup> for 450 °C to 1.28 mmol.g<sup>-1</sup> for 600 °C (Table 2 and Figure 9B). Proportionally, the concentration of Brønsted sites gradually decreased from 1.71 mmol.g<sup>-1</sup> for 450 °C to 1.07 mmol.g<sup>-1</sup> for 600 °C. The Lewis electron acceptor sites are probably formed by step-wise weakening of the bonds in Si–OH–Al Brønsted groups and progressive dehydroxylation with increasing temperatures [54].

The alkylation activity of the series of BEA/4.8 zeolites calcined at different temperatures is depicted in figure 10. The figure clearly shows that the obtained conversions of benzene gradually decrease with increasing calcination temperature. The decrease in the concentration of Brønsted OH groups by their partial transformation to Lewis centres results in a decrease in the activity. The dependence of the benzene conversion on the concentration of Brønsted sites for the series of BEA/4.8 zeolites and the Si-rich BEA/12.5 and BEA/18 zeolite samples is shown in Figure 11A. The data show that the conversion is a function of the concentration of Brønsted sites and the activity increases with the increasing concentration of Brønsted sites regardless of the absence or presence of large numbers of Lewis sites. We also plotted the concentrations of Lewis sites and the conversion of benzene. The plots of the conversion of benzene against the concentrations of the Lewis sites did not show any relationship (Figure 11B). The dependence clearly shows that the activity of the \*BEA zeolite is controlled by the concentration of Brønsted sites and that the Lewis sites do not significantly contribute to the activity.

The effect of the Lewis sites on the selectivity of alkylation was analysed using the series of BEA/4.8 samples providing essentially different ratios between the concentrations of Brønsted and Lewis sites, e.g. ratios of C<sub>B</sub>/C<sub>L</sub> 3.4 and 0.8 for samples calcined at 450 and 600 °C, respectively. The selectivity for EB, DEB and heavier by-products for the samples with the different concentrations of Lewis sites examined at benzene conversion of ~ 15% is shown in

Figure 11C and Table 3. The reaction selectivity for EB is about 95% for all the samples with about 5% DEB and only about 0.5% other by-products. The results clearly show that the Lewis centres do not affect the selectivity of the reaction, at least under the described reaction conditions.

It can be summarised that the benzene conversion increases with an increase in the concentration of acid Brønsted sites regardless of the presence of Lewis sites and the greatest activity with preserved selectivity is observed for samples containing the greatest concentration of the Brønsted sites.

## Conclusions

Analysis of the activity and selectivity with respect to the zeolitic structure and concentration and nature of the acid sites revealed that:

- i) The selectivity for EB is controlled by shape-selectivity effects where a three-dimensional channel structure with 12-membered ring openings of \*BEA zeolite provides high yields of EB without excessive formation of DEB isomers and heavier by-products.
- ii) The concentration of Brønsted acid sites controls the activity of the reaction, while even a very high density of acid sites in \*BEA zeolites does not negatively influence the selectivity of the reaction. Superior activity and selectivity are obtained over Al-rich \*BEA zeolites where the Brønsted OH groups associated with high concentration of Al in the zeolite framework Al-rich \*BEA zeolite represent acidic sites with strength and specific activity comparable or greater compared to Si-rich zeolites.

- iii) Even a very high concentration of the Lewis sites does not contribute to the activity or influence the selectivity of the reaction. The Lewis sites are not involved in the alkylation reaction and play the role of spectators.

It can be concluded that the high concentration of Brønsted OH groups in the shape-selective environment of the 3D channel system associated with a high concentration of Al in the zeolite framework is the decisive factor for the high activity and selectivity in the alkylation reaction.

### Author Contribution Statement

Dr. Faal Rastegar Seyyede Somayeh, Postdoctoral researcher, J. Heyrovsky Institute of Physical Chemistry of the Academy of Sciences of the Czech Republic, Dolejskova 3, Prague 8, Czech Republic, tel.: +(420) 26605 3555, fax: +(420) 28658 2307, e-mail [somayeh.rastegar@jh-inst.cas.cz](mailto:somayeh.rastegar@jh-inst.cas.cz): Kinetic analysis, manuscript preparation.

Dr. Galina Sadovska, Scientist, J. Heyrovsky Institute of Physical Chemistry of the Academy of Sciences of the Czech Republic, Dolejskova 3, Prague 8, Czech Republic, tel.: +(420) 26605 3555, fax: +(420) 28658 2307, e-mail [galina.sadovska@jh-inst.cas.cz](mailto:galina.sadovska@jh-inst.cas.cz). Structural analysis.

Dr. Radim Pilar, Postdoctoral researcher, J. Heyrovsky Institute of Physical Chemistry of the Academy of Sciences of the Czech Republic, Dolejskova 3, Prague 8, Czech Republic, tel.: +(420) 26605 3555, fax: +(420) 28658 2307, e-mail [radim.pilar@jh-inst.cas.cz](mailto:radim.pilar@jh-inst.cas.cz): Synthesis of [petr.sazama@jh-inst.cas.cz](mailto:petr.sazama@jh-inst.cas.cz) zeolites.

Dr. Jaroslava Moravkova, Scientist, J. Heyrovsky Institute of Physical Chemistry of the Academy of Sciences of the Czech Republic, Dolejskova 3, Prague 8, Czech Republic, fax: +(420) 28658 2307, e-mail [jaroslava.moravkova@jh-inst.cas.cz](mailto:jaroslava.moravkova@jh-inst.cas.cz). Microscopic analysis and analytical methods.

Dr. Dalib Kaucky, Senior researcher, J. Heyrovsky Institute of Physical Chemistry of the Academy of Sciences of the Czech Republic, Dolejskova 3, Prague 8, Czech Republic, tel.: +(420) 26605 3775, fax: +(420) 28658 2307, e-mail [dalibor.kaucky@jh-inst.cas.cz](mailto:dalibor.kaucky@jh-inst.cas.cz): Kinetic analysis.

Dr. Libor Brabec, Senior researcher, J. Heyrovsky Institute of Physical Chemistry of the Academy of Sciences of the Czech Republic, Dolejskova 3, Prague 8, Czech Republic, tel.: +(420) 26605 3775, fax: +(420) 28658 2307, e-mail [libor.brabec@jh-inst.cas.cz](mailto:libor.brabec@jh-inst.cas.cz): HR-SEM analysis.

Dr. Jana Pastvova, Postdoctoral researcher, J. Heyrovsky Institute of Physical Chemistry of the Academy of Sciences of the Czech Republic, Dolejskova 3, Prague 8, Czech Republic, tel.: +(420) 26605 3555, fax: +(420) 28658 2307, e-mail [jana.pastvova@jh-inst.cas.cz](mailto:jana.pastvova@jh-inst.cas.cz): FTIR analysis.

Dr. Petr Sazama, Senior scientist, J. Heyrovsky Institute of Physical Chemistry of the Academy of Sciences of the Czech Republic, Dolejskova 3, Prague 8, Czech Republic, tel.: +(420) 26605 3325, fax: +(420) 28658 2307, e-mail [petr.sazama@jh-inst.cas.cz](mailto:petr.sazama@jh-inst.cas.cz): Research management, manuscript preparation.

### Acknowledgments

This work was supported by the Grant Agency of the Czech Republic under Project No. 18-20303S and the Technology Agency of the Czech Republic under Project No. TH03020184. The authors acknowledge the assistance provided by the Research Infrastructure Pro-NanoEnviCz (Project No. CZ.02.1.01/0.0/0.0/16\_013/0001821), supported by the Ministry of Education, Youth and Sports of the Czech Republic.

Journal Pre-proof

**References:**

- [1] T.F. Degnan Jr, C.M. Smith, C.R. Venkat, Alkylation of aromatics with ethylene and propylene: recent developments in commercial processes, *Applied catalysis A: General*, 221 (2001) 283-294.
- [2] C. Perego, P. Ingallina, Combining alkylation and transalkylation for alkylaromatic production, *Green Chemistry*, 6 (2004) 274-279.
- [3] P. Venuto, L.A. Hamilton, P. Landis, J. Wise, Organic reactions catalyzed by crystalline aluminosilicates: I. Alkylation reactions, *Journal of Catalysis*, 5 (1966) 81-98.
- [4] R.A. Innes, S.I. Zones, G.J. Nacamuli, Liquid phase alkylation or transalkylation process using zeolite beta, US4891458, 1990.
- [5] J.C. Cheng, T.F. Degnan, J.S. Beck, Y.Y. Huang, M. Kalyanaraman, J.A. Kowalski, C.A. Loehr, D.N. Mazzone, A comparison of zeolites MCM-22, Beta, and USY for liquid phase alkylation of benzene with ethylene, *Studies in Surface Science and Catalysis*, 121 (1999) 53-60.
- [6] G. Bellussi, G. Pazzuconi, C. Perego, G. Girotti, G. Terzoni, Liquid-phase alkylation of benzene with light olefins catalyzed by  $\beta$ -zeolites, *Journal of Catalysis*, 157 (1995) 227-234.
- [7] J. Cheng, T. Degnan, J. Beck, Y. Huang, M. Kalyanaraman, J. Kowalski, C. Loehr, D. Mazzone, A comparison of zeolites MCM-22, beta, and USY for liquid phase alkylation of benzene with ethylene, *Studies in surface science and catalysis*, Elsevier1999, pp. 53-60.
- [8] A. Corma, V. Martinez-Soria, E. Schnoefeld, Alkylation of benzene with short-chain olefins over MCM-22 zeolite: catalytic behaviour and kinetic mechanism, *Journal of catalysis*, 192 (2000) 163-173.
- [9] A. O'Kelly, J. Kellett, J. Plucker, Monoalkybenzenes by Vapor-Phase Alkylation with Silica-alumina Catalyst, *Industrial & Engineering Chemistry*, 39 (1947) 154-158.
- [10] Y. Shi, E. Xing, W. Xie, F. Zhang, X. Mu, X. Shu, Shape selectivity of beta and MCM-49 zeolites in liquid-phase alkylation of benzene with ethylene, *Journal of Molecular Catalysis A: Chemical*, 418-419 (2016) 86-94.
- [11] Y. Wang, Y. Gao, S. Xie, S. Liu, F. Chen, W. Xin, X. Zhu, X. Li, N. Jiang, L. Xu, Adjustment of the Al siting in MCM-22 zeolite and its effect on alkylation performance of ethylene with benzene, *Catalysis Today*, (2018).

- [12] E. Xing, Y. Shi, W. Xie, F. Zhang, X. Mu, X. Shu, Size-controlled synthesis of MCM-49 zeolite from NaX for liquid-phase alkylation of benzene with ethylene, *Microporous and Mesoporous Materials*, 236 (2016) 54-62.
- [13] S. Lilov, Determination of the effective kinetic diameter of the complex molecules, *Crystal Research and Technology*, 21 (1986) 1299-1302.
- [14] P. Weisz, V. Frilette, Intracrystalline and molecular-shape-selective catalysis by zeolite salts, *The Journal of Physical Chemistry*, 64 (1960) 382-382.
- [15] J. Čejka, B. Wichterlová, ACID-CATALYZED SYNTHESIS OF MONO- AND DIALKYL BENZENES OVER ZEOLITES: ACTIVE SITES, ZEOLITE TOPOLOGY, AND REACTION MECHANISMS, *Catalysis Reviews*, 44 (2002) 375-421.
- [16] B. Xie, J. Song, L. Ren, Y. Ji, J. Li, F.-S. Xiao, Organotemplate-Free and Fast Route for Synthesizing Beta Zeolite, *Chemistry of Materials*, 20 (2008) 4533-4535.
- [17] G. Majano, L. Delmotte, V. Valtchev, S. Mintova, Al-Rich Zeolite Beta by Seeding in the Absence of Organic Template, *Chemistry of Materials*, 21 (2009) 4184-4191.
- [18] Y. Kamimura, S. Tanahashi, K. Itabashi, A. Sugawara, T. Wakihara, A. Shimojima, T. Okubo, Crystallization Behavior of Zeolite Beta in OSDA-Free, Seed-Assisted Synthesis, *The Journal of Physical Chemistry C*, 115 (2011) 744-750.
- [19] B. Yilmaz, U. Muller, M. Feyen, S. Maurer, H. Zhang, X. Meng, F.S. Xiao, X. Bao, W. Zhang, H. Imai, T. Yokoi, T. Tatsumi, H. Gies, T. De Baerdemaeker, D. De Vos, A new catalyst platform: Zeolite Beta from template-free synthesis, *Catal. Sci. Technol.*, 3 (2013) 2580-2586.
- [20] P. Sazama, B. Wichterlová, Š. Sklenák, V.I. Parvulescu, N. Candu, G. Sádovská, J. Dědeček, P. Klein, V. Pashkova, P. Šťastný, Acid and redox activity of template-free Al-rich H-BEA\* and Fe-BEA\* zeolites, *Journal of Catalysis*, 318 (2014) 22-33.
- [21] B. Wichterlová, Z. Tvarůžková, Z. Sobalík, P. Sarv, Determination and properties of acid sites in H-ferrierite: A comparison of ferrierite and MFI structures, *Microporous and Mesoporous Materials*, 24 (1998) 223-233.
- [22] P. Sazama, E. Tabor, P. Klein, B. Wichterlova, S. Sklenak, L. Mokrzycki, V. Pashkova, M. Ogura, J. Dedeczek, Al-rich beta zeolites. Distribution of Al atoms in the framework and related protonic and metal-ion species, *Journal of Catalysis*, 333 (2016) 102-114.

- [23] J. Pastvova, R. Pilar, J. Moravkova, D. Kaucky, J. Rathousky, S. Sklenak, P. Sazama, Tailoring the structure and acid site accessibility of mordenite zeolite for hydroisomerisation of n-hexane, *Applied Catalysis A: General*, 562 (2018) 159-172.
- [24] R. Gounder, E. Iglesia, Effects of partial confinement on the specificity of monomolecular alkane reactions for acid sites in side pockets of mordenite, *Angewandte Chemie - International Edition*, 49 (2010) 808-811.
- [25] A. Bhan, E. Iglesia, A link between reactivity and local structure in acid catalysis on zeolites, *Acc. Chem. Res.*, 41 (2008) 559-567.
- [26] H. Chiang, A. Bhan, Catalytic consequences of hydroxyl group location on the kinetics of n-hexane hydroisomerization over acidic zeolites, *J. Catal.*, 283 (2011) 98-107.
- [27] N. Wang, M. Zhang, Y. Yu, Distribution of aluminum and its influence on the acid strength of Y zeolite, *Microporous Mesoporous Mater.*, 169 (2013) 47-53.
- [28] P. Sazama, D. Kaucky, J. Moravkova, R. Pilar, P. Klein, J. Pastvova, E. Tabor, S. Sklenak, I. Jakubec, L. Mokrzycki, Superior activity of non-interacting close acidic protons in Al-rich Pt/H-\*BEA zeolite in isomerization of n-hexane, *Applied Catalysis A: General*, 533 (2017) 28-37.
- [29] M. Boronat, A. Corma, What Is Measured When Measuring Acidity in Zeolites with Probe Molecules?, *ACS Catalysis*, 9 (2019) 1539-1548.
- [30] R. Gounder, E. Iglesia, The catalytic diversity of zeolites: confinement and solvation effects within voids of molecular dimensions, *Chemical Communications*, 49 (2013) 3491-3509.
- [31] J. Pastvova, D. Kaucky, J. Moravkova, J. Rathousky, S. Sklenak, M. Vorokhta, L. Brabec, R. Pilar, I. Jakubec, E. Tabor, P. Klein, P. Sazama, Effect of Enhanced Accessibility of Acid Sites in Micromesoporous Mordenite Zeolites on Hydroisomerization of n-Hexane, *ACS Catalysis*, 7 (2017) 5781-5795.
- [32] A.N.C. van Laak, R.W. Gosselink, S.L. Sagala, J.D. Meeldijk, P.E. de Jongh, K.P. de Jong, Alkaline treatment on commercially available aluminum rich mordenite, *Applied Catalysis A: General*, 382 (2010) 65-72.
- [33] W. Vermeiren, J.P. Gilson, Impact of Zeolites on the Petroleum and Petrochemical Industry, *Topics in Catalysis*, 52 (2009) 1131-1161.

- [34] T. De Baerdemaeker, B. Yilmaz, U. Muller, M. Feyen, F.S. Xiao, W. Zhang, T. Tatsumi, H. Gies, X. Bao, D. De Vos, Catalytic applications of OSDA-free Beta zeolite, *J. Catal.*, 308 (2013) 73-81.
- [35] P. Sazama, J. Pastvova, D. Kaucky, J. Moravkova, J. Rathousky, I. Jakubec, G. Sadovska, Does hierarchical structure affect the shape selectivity of zeolites? Example of transformation of n-hexane in hydroisomerization, *Journal of Catalysis*, 364 (2018) 262-270.
- [36] B. Xie, H. Zhang, C. Yang, S. Liu, L. Ren, L. Zhang, X. Meng, B. Yilmaz, U. Muller, F.-S. Xiao, Seed-directed synthesis of zeolites with enhanced performance in the absence of organic templates, *Chem. Commun. (Cambridge, U. K.)*, 47 (2011) 3945-3947.
- [37] S. Suganuma, H. Zhang, C. Yang, F.S. Xiao, N. Katada, Acidic property of BEA zeolite synthesized by seed-directed method, *J Porous Mater*, 23 (2016) 415-421.
- [38] P. Sazama, L. Mokrzycki, B. Wichterlova, A. Vondrova, R. Pilar, J. Dedecek, S. Sklenak, E. Tabor, Unprecedented propane-SCR-NO<sub>x</sub> activity over template-free synthesized Al-rich Co-BEA\* zeolite, *Journal of Catalysis* 332 (2015) 201-211.
- [39] P. Sazama, B. Wichterlova, S. Sklenak, V.I. Parvulescu, N. Candu, G. Sadovska, J. Dedecek, P. Klein, V. Pashkova, P. Stastny, Acid and redox activity of template-free Al-rich H-BEA\* and Fe-BEA\* zeolites, *J. Catal.*, 318 (2014) 22-33.
- [40] P. Sazama, R. Pilar, L. Mokrzycki, A. Vondrova, D. Kaucky, J. Plsek, S. Sklenak, P. Stastny, P. Klein, Remarkably enhanced density and specific activity of active sites in Al-rich Cu-, Fe- and Co-beta zeolites for selective catalytic reduction of NO<sub>x</sub>, *Appl. Catal., B.*, 189 (2016) 65-74.
- [41] P.J. Kunkeler, B.J. Zuurdeeg, J.C. van der Waal, J.A. van Bokhoven, D.C. Koningsberger, H. van Bekkum, Zeolite Beta: The Relationship between Calcination Procedure, Aluminum Configuration, and Lewis Acidity, *Journal of Catalysis*, 180 (1998) 234-244.
- [42] R. Weingarten, G.A. Tompsett, W.C. Conner Jr, G.W. Huber, Design of solid acid catalysts for aqueous-phase dehydration of carbohydrates: The role of Lewis and Brønsted acid sites, *Journal of Catalysis*, 279 (2011) 174-182.
- [43] E.J. Creighton, S.D. Ganeshie, R.S. Downing, H. Van Bekkum, Stereoselective Meerwein-Ponndorf-Verley and Oppenauer reactions catalysed by zeolite BEA, *Journal of Molecular Catalysis A: Chemical*, 115 (1997) 457-472.

- [44] P. Sazama, B. Wichterlova, J. Dedecek, Z. Tvaruzkova, Z. Musilova, L. Palumbo, S. Sklenak, O. Gonsiorova, FTIR and  $^{27}\text{Al}$  MAS NMR analysis of the effect of framework Al- and Si-defects in micro- and micro-mesoporous H-ZSM-5 on conversion of methanol to hydrocarbons, *Microporous and Mesoporous Materials*, 143 (2011) 87-96.
- [45] S. Müller, Y. Liu, F.M. Kirchberger, M. Tonigold, M. Sanchez-Sanchez, J.A. Lercher, Hydrogen Transfer Pathways during Zeolite Catalyzed Methanol Conversion to Hydrocarbons, *Journal of the American Chemical Society*, 138 (2016) 15994-16003.
- [46] O. Bortnovsky, P. Sazama, B. Wichterlova, Cracking of pentenes to C2-C4 light olefins over zeolites and zeotypes: Role of topology and acid site strength and concentration, *Applied Catalysis A: General*, 287 (2005) 203-213.
- [47] Y. Zhang, R. Zhao, M. Sanchez-Sanchez, G.L. Haller, J. Hu, R. Bermejo-Deval, Y. Liu, J.A. Lercher, Promotion of protolytic pentane conversion on H-MFI zeolite by proximity of extra-framework aluminum oxide and Brønsted acid sites, *Journal of Catalysis*, 370 (2019) 424-433.
- [48] N. Xue, A. Vjunov, S. Schallmoser, J.L. Fulton, M. Sanchez-Sanchez, J.Z. Hu, D. Mei, J.A. Lercher, Hydrolysis of zeolite framework aluminum and its impact on acid catalyzed alkane reactions, *Journal of Catalysis*, 365 (2018) 359-366.
- [49] R. Gounder, A.J. Jones, R.T. Carr, E. Iglesia, Solvation and acid strength effects on catalysis by faujasite zeolites, *Journal of Catalysis*, 286 (2012) 214-223.
- [50] C. Perego, P. Ingallina, Recent advances in the industrial alkylation of aromatics: new catalysts and new processes, *Catalysis Today*, 73 (2002) 3-22.
- [51] S. Kotrel, M.P. Rosynek, J.H. Lunsford, Quantification of Acid Sites in H-ZSM-5, H- $\beta$ , and H-Y Zeolites, *Journal of Catalysis*, 182 (1999) 278-281.
- [52] I. Kiricsi, C. Flego, G. Pazzuconi, W.O. Parker, Jr., R. Millini, C. Perego, G. Bellussi, Progress toward Understanding Zeolite .beta. Acidity: An IR and  $^{27}\text{Al}$  NMR Spectroscopic Study, *The Journal of Physical Chemistry*, 98 (1994) 4627-4634.
- [53] L. Čapek, J. Dědeček, P. Sazama, B. Wichterlová, The decisive role of the distribution of Al in the framework of beta zeolites on the structure and activity of Co ion species in propane-SCR-NO<sub>x</sub> in the presence of water vapour, *Journal of Catalysis*, 272 (2010) 44-54.
- [54] J. Brus, L. Kobera, W. Schoefberger, M. Urbanová, P. Klein, P. Sazama, E. Tabor, S. Sklenak, A.V. Fishchuk, J. Dědeček, Structure of framework aluminum lewis sites and perturbed

aluminum atoms in zeolites as determined by  $^{27}\text{Al}\{^1\text{H}\}$  REDOR (3Q) MAS NMR spectroscopy and DFT/molecular mechanics, *Angewandte Chemie - International Edition*, 54 (2015) 541-545.

Journal Pre-proof

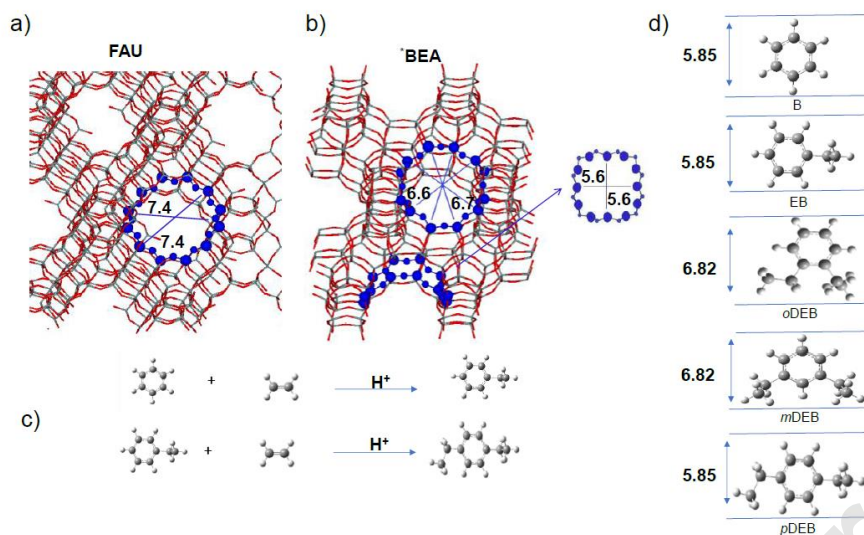


**Figure 1.** The channel structure and diameters of the openings of the 12-membered rings in the structure of a) FAU and b) \*BEA zeolites, c) the reaction scheme for alkylation of benzene to EB and DEB, and d) the kinetic diameters of the benzene, EB and DEB isomers. The kinetic diameters of the DEB isomers were calculated based on the work of Lilov et al. [13]. The data are in Å.

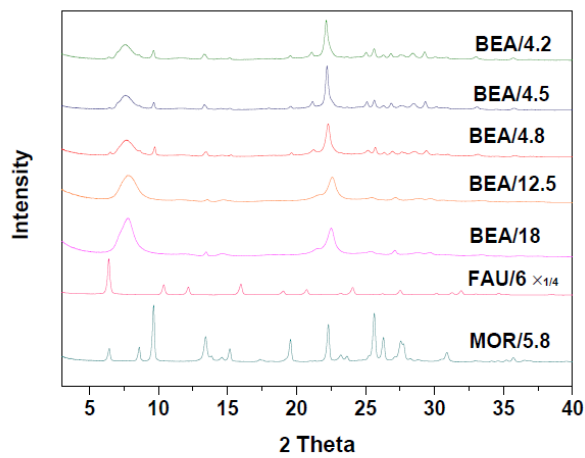


**Figure 2.** X-ray diffraction patterns of the \*BEA, FAU and MOR zeolites.

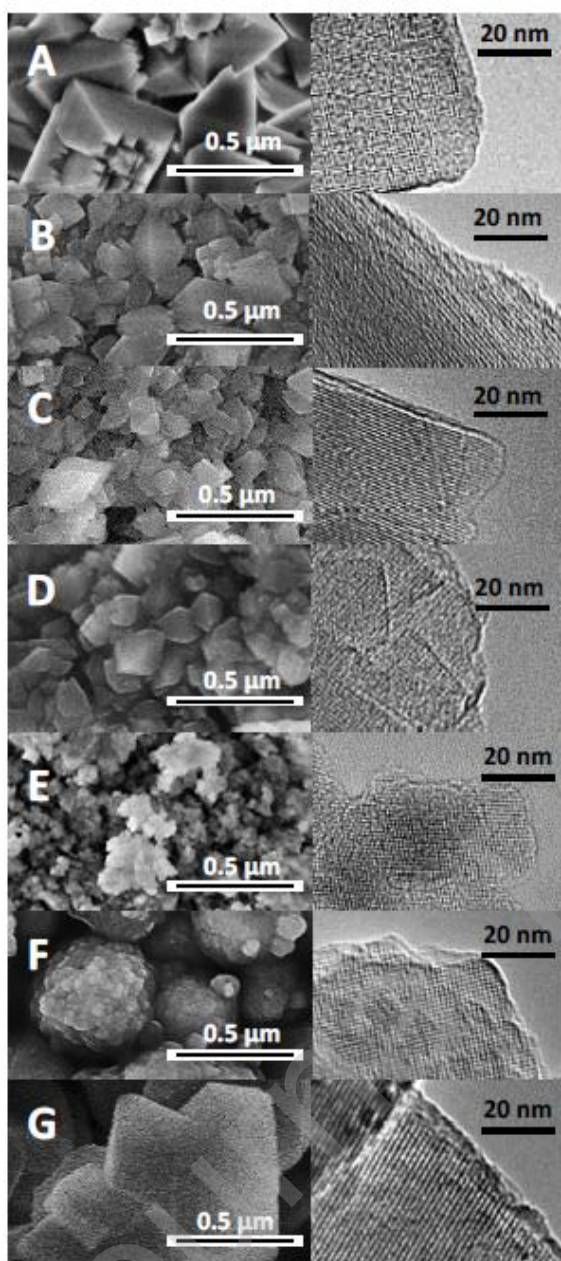


**Figure 3.** SEM and HR-TEM micrographs for zeolites BEA/4.2 (A), BEA/4.5 (B), BEA/4.8 (C), BEA/5 (D), BEA/12 (E), BEA/18 (F), and USY/6 (G).

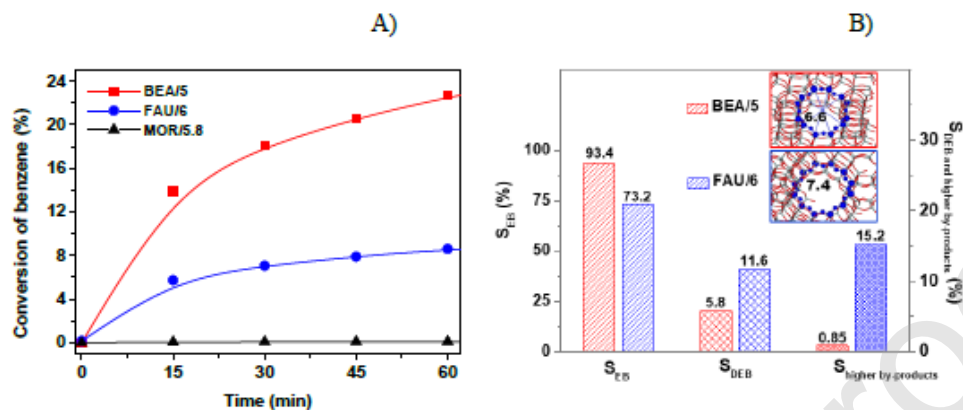


**Figure 4.** Effect of the zeolitic structure on alkylation of benzene with ethylene over Al-rich

\*BEA, MOR and FAU with similar framework compositions. A) Conversion of benzene as a function of time. B) The comparison of selectivity of Al-rich \*BEA with FAU zeolite for EB, DEB and heavier by-products ( $C \geq 9$ ) at similar conversions of benzene  $\sim 15\%$ .

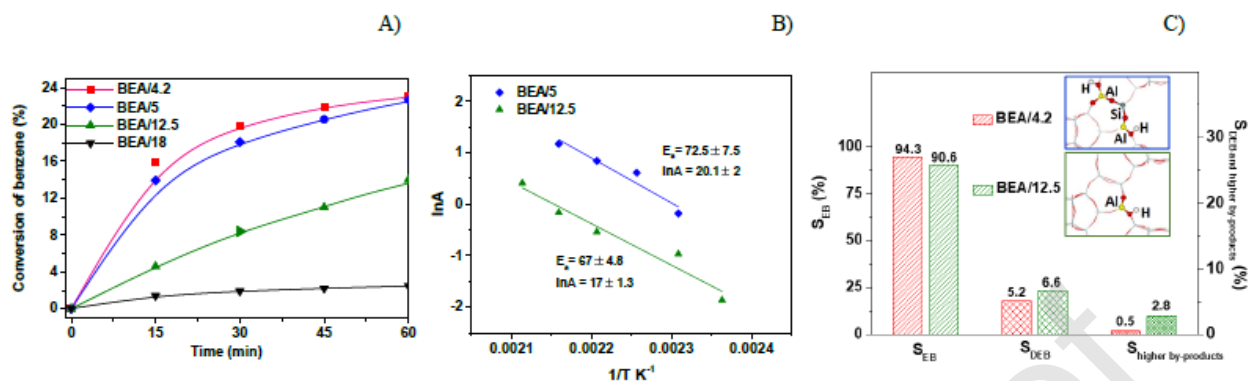


**Figure 5.** Effect of the Si/Al ratio of \*BEA zeolite catalysts on the activity in the alkylation of benzene with ethylene. A) Conversion of benzene as a function of time and B) the Arrhenius plot with the determined pre-exponential factors  $\ln(A)$  and activation energies. C) The comparison of the selectivity of Al-rich and Si-rich \*BEA zeolites for EB, DEB and heavier by-products ( $C \geq 9$ ) at similar conversions of benzene ~ 15%.

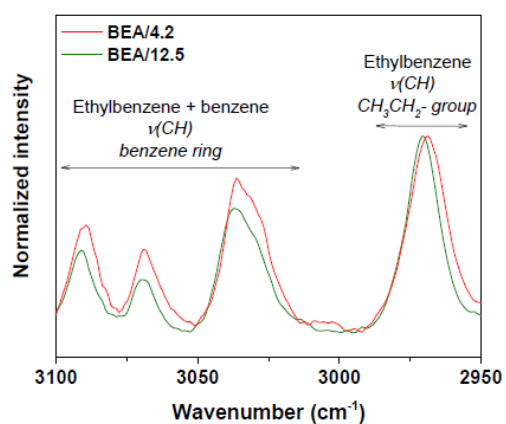


**Figure 6.** FTIR analysis of competitive adsorption of benzene and EB on Al-rich (H-BEA/4.2) and Si-rich (H-BEA/12.5) beta zeolites. The spectrum of Al-rich \*BEA zeolite shows higher intensity of the bands of the benzene ring at the same intensity of the bands of the ethyl group on both zeolites.

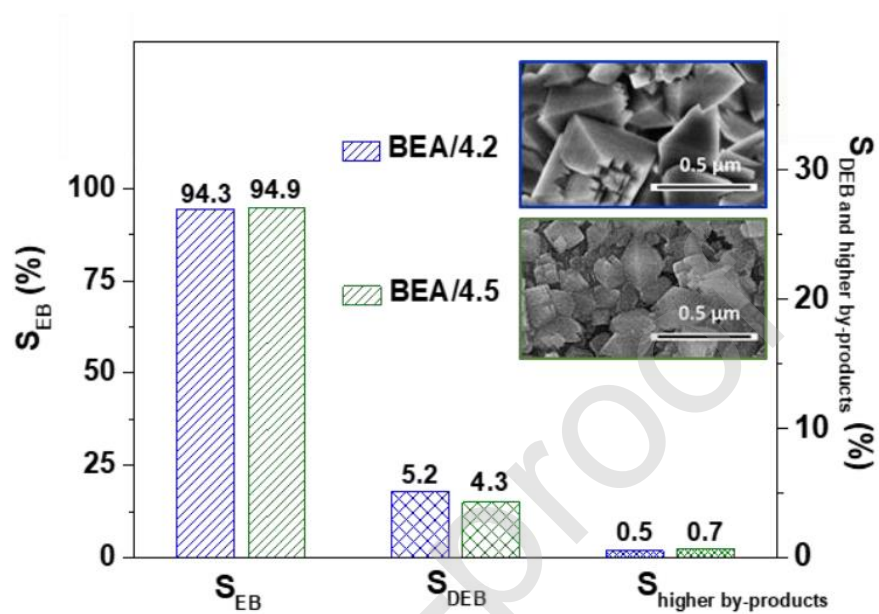


**Figure 7.** Illustration of negligible effects of the crystal size on the selectivity in the alkylation of benzene with ethylene over Al-rich \*BEA zeolites differing in the crystal size.

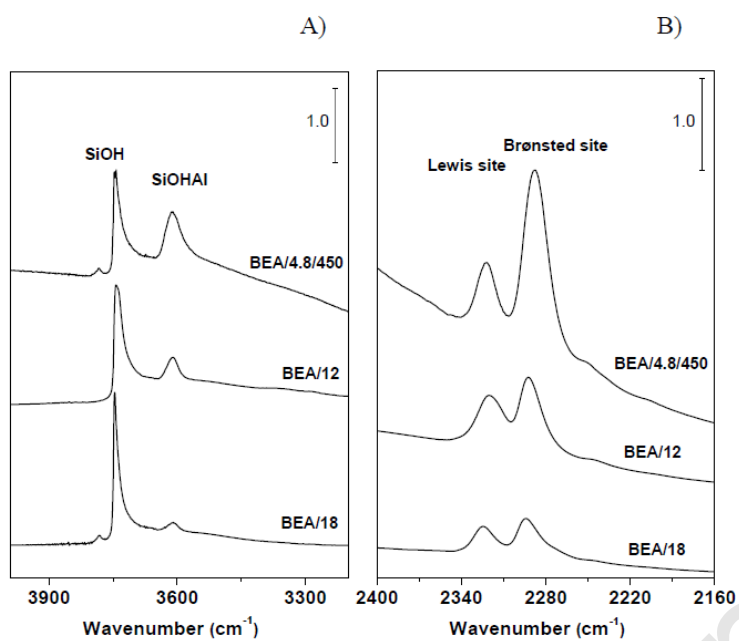


**Figure 8.** Analysis of acidity using FTIR spectra of Al- and Si-rich H<sup>\*</sup>-BEA zeolites. A) The region of the OH groups (ν(O-H)) and

B) the ν(C≡N) region after adsorption of d<sub>3</sub>-acetonitrile.

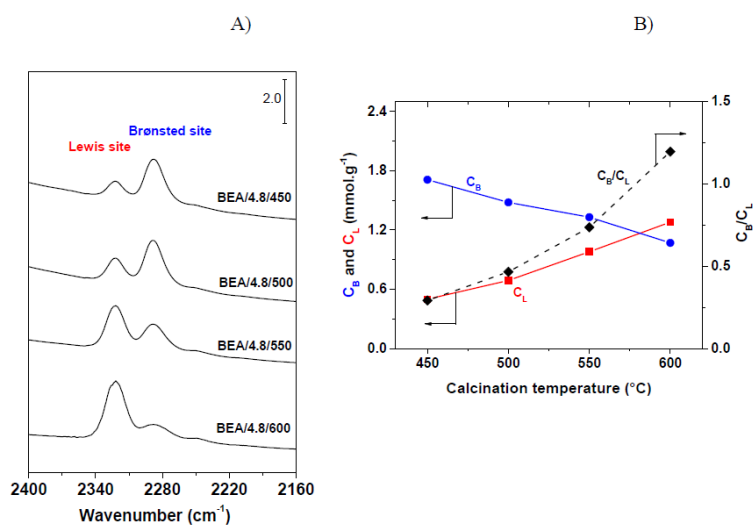


**Figure 9.** FTIR analysis of the Brønsted and Lewis acidity for Al-rich  $^*\text{BEA}/4.8$  zeolites calcined at 450 – 600 °C. A) The  $\nu(\text{C}\equiv\text{N})$  region after adsorption of  $d_3$ -acetonitrile and B) the effect of the calcination temperature on the concentrations of the Brønsted and Lewis acid sites.

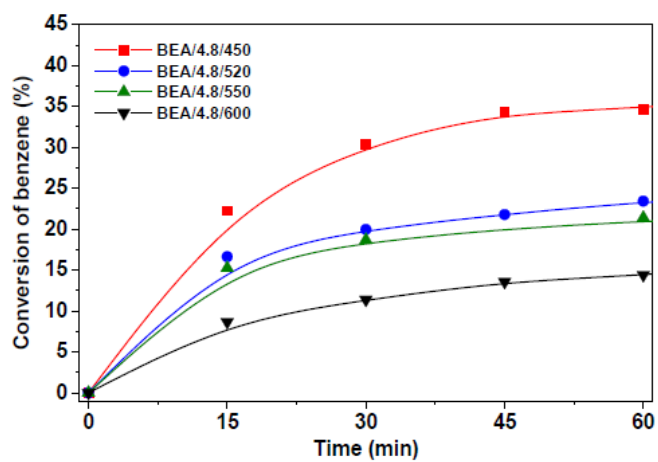


**Figure 10.** Effect of the calcination temperature on the activity in the alkylation of benzene with ethylene over BEA/4.8 treated at 450 – 600 °C.

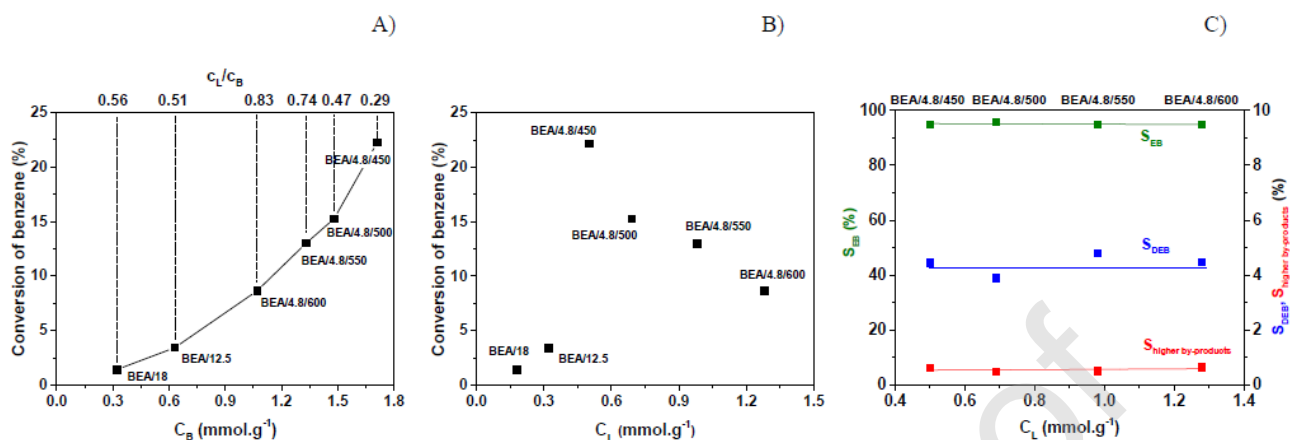


**Figure 11.** Analysis of the role of Brønsted and Lewis acid sites in the alkylation of benzene with ethylene over \*BEA zeolites: A) Conversion of benzene as a function of the concentration of the Brønsted acid sites. The conversion regularly increases with the concentration of Brønsted sites regardless of the various contents of the Lewis sites and  $c_L/c_B$  ratios. B) The plot of the conversions of benzene against the concentrations of the Lewis sites. The data do not show any relationship. C) The same selectivity for EB ( $S_{EB}$ ), DEB ( $S_{DEB}$ ) and higher by-products analysed at benzene conversion  $\sim 15\%$  over the series of BEA/4.8 zeolites largely differing in the concentration of Lewis sites.

**Table 1.** Characteristics of the zeolites.

Sample	Si/Al ratio	Crystal size $\mu\text{m}$	$V_{\text{MI}}$ $\text{cm}^3 \text{g}^{-1}$	$S_{\text{EXT}}$ $\text{m}^2 \cdot \text{g}^{-1}$
BEA/4.2	4.2	0.4–0.5	0.20	58
BEA/4.5	4.5	0.1–0.2	0.16	138
BEA/4.8	4.8	0.1–0.3	-	-
BEA/5	5.0	0.1–0.2	0.16	113
BEA/12.5	12.5	0.01–0.1	0.19	244
BEA/18	18	0.05–0.1	0.15	220
MOR/5.8	5.8	0.1–1	0.16	31
FAU/6	6.0	0.3–0.5	0.33	52

**Table 2.** Concentrations of Brønsted and Lewis sites for Al-rich \*BEA calcined at temperatures 450 – 600 °C and Al-rich MOR and Si-rich \*BEA zeolites.

Sample	Si/Al	C <sub>B</sub> <sup>a</sup>	C <sub>L</sub> <sup>a</sup>	C <sub>B</sub> /C <sub>L</sub>
		mmol.g <sup>-1</sup>		
MOR/5.8	5.8	0.97	0.45	2.2
BEA/12.5	12.5	0.63	0.32	2.0
BEA/18	18	0.32	0.18	1.8
BEA/4.8/450	4.8	1.71	0.50	3.4
BEA/4.8/500	4.8	1.48	0.69	2.1
BEA/4.8/550	4.8	1.33	0.98	1.4
BEA/4.8/600	4.8	1.07	1.28	0.8

<sup>a</sup> Concentrations of acid Brønsted and Lewis sites, respectively, from FTIR spectra of adsorbed *d*<sub>3</sub>-acetonitrile.

**Table 3.** Negligible effect of Lewis sites on selectivity for EB, DEB and heavier by-products ( $C \geq 10$ ) in the reaction of alkylation benzene with ethene over the BEA/4.8 calcined at different temperatures. Selectivity at benzene conversion  $\sim 15\%$ .

Zeolite	$C_B/C_L$	$S_{EB}$	$S_{DEB}$	$S_{\text{higher by-products}}$
		%		
BEA/4.8/450	3.4	94.92	4.45	0.62
BEA/4.8/500	2.1	95.63	3.89	0.48
BEA/4.8/520	-	93.65	5.81	0.54
BEA/4.8/550	1.4	94.71	4.79	0.50
BEA/4.8/600	0.8	94.89	4.46	0.65